Polyimides with a Diazo Chromophore Exhibiting High Thermal Stability and Large Electrooptic Coefficients

Haythem Saadeh, Alireza Gharavi, Dong Yu, and Luping Yu*

Department of Chemistry and The James Frank Institute, The University of Chicago, 5735 South Ellis Avenue, Chicago, Illinois 60637

Received April 18, 1997; Revised Manuscript Received June 25, 1997[⊗]

ABSTRACT: To synthesize nonlinear optical polyimides exhibiting high nonlinearity and high thermal stablity, a new monomer bearing phenylenediamine and a diazo benzene-type nonlinear optical chromophore (compound **1**) was synthesized and polymerized with 4,4′-(hexafluoroisopropylidene)diphthalic anhydride. This diazo chromophore possesses a microscopic optical nonlinearity larger than either the Disperse Red 1 or DANS chromophores. Copolymerization of compound **1** and 1,4-diaminophenylene with 4,4′-(hexafluoroisopropylidene)diphthalic anhydride yielded copolyimides with higher glass transition temperatures. These polyimides exhibit large electrooptic coefficients, $r_{33} \sim 14-35$ pm/V. The second harmonic measurements indicate long-term stability of the dipole orientation (>800 h at 100 °C) for these polyimides.

Introduction

Over the past 3 years, we have synthesized numerous polyimides functionalized with nonlinear optical (NLO) chromophores.[1−4] Their second-order NLO properties have been studied in detail. The motivation, of course, stemmed from an interest in developing novel polymeric materials with large nonlinear optical (NLO) responses and a stable dipole orientation. It is known that larger nonlinear optical (NLO) responses and a higher thermal stablility in dipole orientation are two key requirements in the development of second-order NLO materials for practical application.[1−6] The polyimide backbones were chosen because of their high glass transition temperatures, which are needed to fix the dipole orientation of the NLO chromophores induced by an external electric field. Research efforts focusing on functionalized polyimides for NLO studies are also performed by other groups, and significant progress has been made.[5−9] However, most of these efforts have resulted in polyimides incorporating NLO chromophores that are easily synthesized and not very sensitive toward chemical manipulation, such as Disperse Red 1 ($\mu\beta(1.3\,\mu m) = 751 \times 10^{-31}$ esu) and DANS ($\mu\beta(1.3\,\mu m) = 662 \times 10^{-31}$ esu). Although these materials exhibit high stability, their optical nonlinearity is still not high enough to compete with inorganic materials, such as $LiNbO_3$. This paper reports our efforts to extend our previous work in order to incorporate NLO chromophores with large $\mu\beta$ values. The combination of the polyimide backbone with a chromophore of high molecular nonlinearity (β) is expected to result in a high-performance polymeric system for electrooptic applications. The versatility of the synthetic approach developed in our laboratory allows us to do so without great difficulty.[1−4] Chromophore **1** was chosen as the NLO moiety to be incorporated. It contains three benzene rings connected with azo groups (diazo dye) and exhibits a $\mu\beta$ value of 4600×10^{-31} esu at 1.3 μm, which is many times higher than the $\mu\beta$ value of either Disperse Red 1 or tricyanovinyl chromophores.[10,11]

The higher nonlinearity of this diazo chromophore is attributed to its longer conjugation length. However, the long conjugation has also resulted in a major side

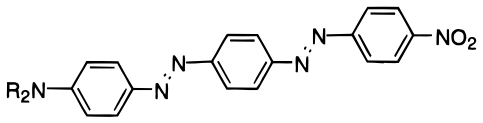

Chromophore 1

effect: depression of the glass transition temperature due to its stronger plasticizing effect. We observed that polyimides functionalized by NLO chromophores exhibit glass transition temperatures lower than nonfunctionalized polyimides. Recently, we demonstrated that if a diamino monomer bearing an NLO chromophore is copolymerized with 1,4-phenylenediamine and the corresponding dianhydride, NLO copolyimides with higher glass transition temperatures can be synthesized.[4] It must be pointed out that these copolyimides also have a tradeoff on nonlinearity because of the decrease of the NLO chromophore concentration. To strike a balance between the thermal stability and optical nonlinearity, the incorporation of an NLO chromophore, with a large β value, into copolyimides will be an interesting approach. This paper reports the detailed synthesis and characterization of different polyimides bearing chromophore **1**. It was found that these polyimides exhibit high optical nonlinearity and a reasonably high glass transition temperature. Temporal measurements also showed stability of nonlinearity at elevated temperatures (e.g., at 100 °C) beyond 800 h.

Experimental Section

Methylene chloride was purified by distillation over calcium hydride. 4,4′-(Hexafluoroisopropylidene)diphthalic anhydride was purified by recrystallization from acetic anhydride and dried under vacuum at 150 °C. 1,4-Phenylenediamine was recrystallized from benzene. All other chemicals were purchased from Aldrich Chemical Co. and were used as received unless otherwise stated. The numbering of the compounds is shown in Scheme 1.

Compound 4. Compound **2**[3] (4.00 g, 10.4 mmol) was completely dissolved in 50 mL of anhydrous NMP under nitrogen. After the addition of *N*-ethyl-*N*-(β-hydroxyethyl)-analine (**3**) (1.88 g, 11.43 mmol) and triphenylphosphine (3.00 g, 15.6 mmol), diethyl azodicarboxylate (2.00 g, 15.6 mmol) in 5 mL of anhydrous NMP was added dropwise. The reaction mixture was stirred at room temperature for 3 h and then precipitated into 150 mL of methanol. The product was

[⊗] Abstract published in *Advance ACS Abstracts,* August 15, 1997.

S0024-9297(97)00530-5 CCC: $14.00

collected by filtration and recrystallized from chloroform/MeOH to give compound **4** as yellow crystals (4.00 g, 73%, 224−225 °C). ^{1}H NMR ($CDCl_3$ ppm): δ 7.96 (m, 4 H, phthalimide protons), 7.85 (m, 4 H, phthalimid protons), 7.40 (d, J = 8.5 Hz, 1 H, ArH), 7.25 (m, 2 H, ArH), 7.10 (m, 2 H, ArH), 6.5−6.7 (m, 2 H, ArH), 4.20 (t, J = 6.0 Hz, 2 H, $-OCH_2CH_2N-$), 3.61 (t, J = 5.6 Hz, 2 H, $-NCH_2CH_2O-$), 3.26 (q, J = 6.8 Hz, 2 H, $-NCH_2CH_3$), 1.00 (t, J = 5.6 Hz, 3 H, $-NCH_2CH_3$).

Compound 6. Disperse Red **5** (1.1 g, 4.54 mmol) was dissolved in 85% phosphoric acid (40 mL), and the solution was cooled to 0 °C. The resulting solution was then treated with a solution of sodium nitrite (0.32 g in 5 mL of H_2O) dropwise while being stirred. After the addition was completed, the solution was allowed to stir for 15 min and was then added in portion into a solution of compound **4** (2.40 g, 4.50 mmoL) in DMF (50 mL). The solution was stirred for 2 h and was then treated with cold water (25 mL). The precipitate was collected by filtration and then recrystallized from NMP/H_2O to give compound **6** as a black-purple solid (1.42 g, 50% 210−212 °C dec). ^{1}H NMR ($CDCl_3$/DMSO, ppm) δ: 8.33 (d, J = 8.5 Hz, ArH, 2H), 8.00 (m, phthalimide protons, 4H), 7.91 (m, phthalimid protons, 4H), 7.80 (d, J = 7.2 Hz, ArH, 2H), 7.74 (d, J = 7.8 Hz, ArH, 2H), 7.63 (d, J = 7.5 Hz, ArH, 2H), 7.58 (d, J = 7.2 Hz, ArH, 2H), 7.33 (d, J = 7.2 Hz, ArH, 2H), 6.63 (d, J = 8.1 Hz, ArH, 2H), 4.25 (t, J = 5.2 Hz, $-OCH_2CH_2N-$, 2H), 3.70 (t, J = 5.2 Hz, $-NCH_2CH_2O-$, 2H), 3.36 (q, J = 7.2 Hz, $-NCH_2CH_3$, 2H), 1.09 (t, J = 6.8 Hz, 3H, $-NCH_2CH_3$).

Compound 7. To a two-necked flask containing compound **6** (0.80 g, 0.892 mmol) and THF (35 mL) was added hydrazine hydrate (25 mL). The solution was stirred at room temperature for 1 h under nitrogen. Water was added to the reaction mixture and then extracted with $CHCl_3$ (2 × 34 mL). The organic layer was concentrated, MeOH was added, and a black product crystallized out. The crude product was recrystallized from $CHCl_3$/MeOH to yield compound **7** (0.185 g, 40%, mp 208−210 °C dec). ^{1}H NMR ($CDCl_3$, ppm): δ 8.31 (d, J = 8.5 Hz, ArH, 2H), 8.00 (m, ArH, 4H), 7.93 (d, J = 8.0 Hz, ArH, 2H), 7.86 (d, J = 8.8 Hz, ArH, 2H), 6.52 (d, J = 8.1 Hz, ArH, 1H), 6.19 (s, ArH, 1H), 6.16 (d, J = 8.0 Hz, ArH, 1H), 4.15 (t, J = 5.2 Hz, $-NCH_2CH_2O-$, 2H), 3.85 (t, J = 5.2 Hz, $-NCH_2CH_2O-$, 2H), 3.57 (q, J = 7.2 Hz, $-NCH_2CH_3$, 2H), 3.31 (s, $ArNH_2$, 4H), 1.27 (t, J = 7.0 Hz, $-NCH_2CH_3$, 3H). Anal. Calcd for $C_{28}H_{28}N_8O_3$: C, 64.11; H, 5.38; N, 21.36. Found: C, 64.16; H, 5.33; N, 21.44.

Polymerization. Compound **7** (0.16 g, 0.313 mmol) was dissolved in 2.5 mL of anhydrous NMP at room temperature, followed by the addition of dianhydride **8** (0.138 g, 0.313 mmol). The solution was stirred at room temperature for 12 h. A mixture of acetic anhydride and pyridine (6 mL/3 mL, 2:1) was added to the reaction solution at room temperature. The resultant mixture was stirred for 2 h and then heated to 90 °C for 3 h. The polymer was precipitated into methanol (75 mL) and collected by filtration. The solid was further purified by dissolving in 1,1,2,2-tetrachloroethane (TCE) and reprecipitated into methanol. The polymer was collected and washed with methanol in a Soxhlet extractor for 24 h and then dried under vacuum at 60 °C for 24 h. ^{1}H NMR ($CDCl_3$, ppm): δ 8.30 (s, ArH, 2H), 7.93 (m, ArH, 12H), 7.75 (s, ArH, 1H), 7.65 (s, ArH, 2H), 7.35 (s, ArH, 1H), 7.20 (s, ArH, 1H), 6.65 (s, ArH, 2H), 4.25 (s, $-NCH_2CH_2O-$, 2H), 3.70 (s, $-NCH_2CH_2O-$, 2H), 3.35 (s, $-NCH_2CH_3$, 2H), 1.10 (s, $-CH_2CH_3$, 3H). Anal. Calcd for $C_{47}H_{30}N_8O_7F_6$: C, 60.52; H, 3.24; N, 12.01. Found: C, 60.27; H, 3.29; N, 11.95.

The above polymerization procedure exemplifies the synthesis of copolyimides **P2** and **P3** where a stoichiometric amount of 1,4-phenylenediamine was added. The ^{1}H NMR spectra of **P2** and **P3** are similar except for the relative magnitude of the peaks.

P2. Anal. Calcd for $C_{39.66}H_{23.33}N_6F_6O_6$: C, 59.78; H, 2.98; N, 10.88. Found: C, 59.93; H, 3.10; N, 10.55.

P3. Anal. Calcd for $C_{36}H_{20}N_5F_6O_{5.5}$: C, 59.68; H, 2.78; N, 9.67. Found: C, 59.49; H, 2.86; N, 9.60.

Characterization. The ^{1}H NMR spectra were recorded on a Varian 500-MHz FT NMR spectrometer. UV−visible spectra were recorded using a Shimadzu UV-240IPC spectrophotometer. The GPC measurements were performed on a Waters RI system equipped with a UV detector and a differential refractometer detector, using THF as an eluent. The molecular weight distributions were calculated on the basis of monodispersed polystyrene standards. Thermal analyses were performed using the DSC-10 and TGA-50 systems from TA instruments under a nitrogen atmosphere. The melting points were obtained with open capillary tubes on a Mel-Temp apparatus. Elemental analyses were performed by Atlantic Microlab, Inc.

Scheme 1. Synthesis of Monomer

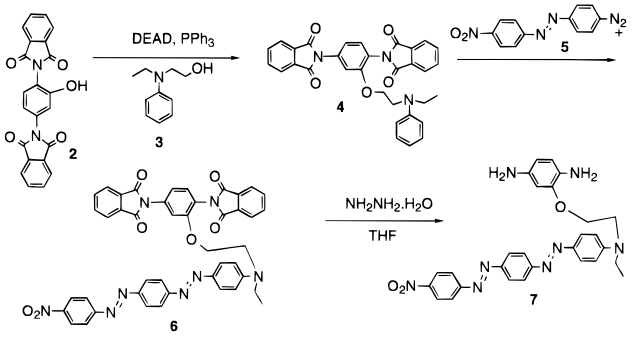

Optical Measurement. We performed the Teng and Man ellipsometric technique for the electrooptic coefficient measurements.[12] For these measurements, a casted polymer sample on an indium−tin−oxide (ITO) substrate was poled under a corona discharge at 200 °C. While the corona discharge was maintained, the sample was cooled to room temperature. Silver electrodes (0.1 micron thick) were evaporated on the polymer surface. The thickness and refractive index measurements were performed by a prizm-coupler from Metricon.

The second harmonic generation (SHG) of the poled polymeric films was measured by using a model-locked Nd:YAGlaser (Continuum-PY61C-10 with a pulse width of 25 ps and a repetition rate of 10 Hz) as a fundamental source (1.064 μm). A quartz crystal was used as the reference sample.

Results and Discussion

Monomer Synthesis. The overall pathway of the monomer synthesis is a modification of our previous work.[3] The synthesis of diamino monomer **7** bearing chromophore **1** is outlined in Scheme 1. The synthesis starts by utilizing the coupling reaction between the diazonium salt of Disperse Red 5 with a solution of compound **4** in DMF, whence upon the addition of H_2O, the product precipitated out and separated by filtration. The aminolysis of diimido **6** with hydrazine hydrate yielded the corresponding diamino monomer **7**. ^{1}H-NMR and elemental analysis showed that pure monomers were obtained.

Polymerization and Characterization. The polymers were synthesized by reacting aromatic dianhydride with stoichiometric amounts of diamine monomers (Scheme 2). The polycondensation reaction was carried in NMP at room temperature in two steps: (1) polymerization of diaminno monomer **7** with dianhydride **8** to give polyamic acid; (2) in-situ imidization of the resulting polyamic acid solution by a Ac_2O/pyridine solution (2:1). The hexafluoroisopropylidene dianhydride **8** was used as a monomer in polymerization in order to enhance the solubility of the corresponding polymers in common organic solvents (THF, DMF, DMSO, and so on). The molecular weights were determined using GPC using polystyrene as the standard and THF as the eluent: the results are shown in Table 1. High molecular weights were obtained for polyimides **P2** and **P3** (123 and 144 kDa, respectively). The large

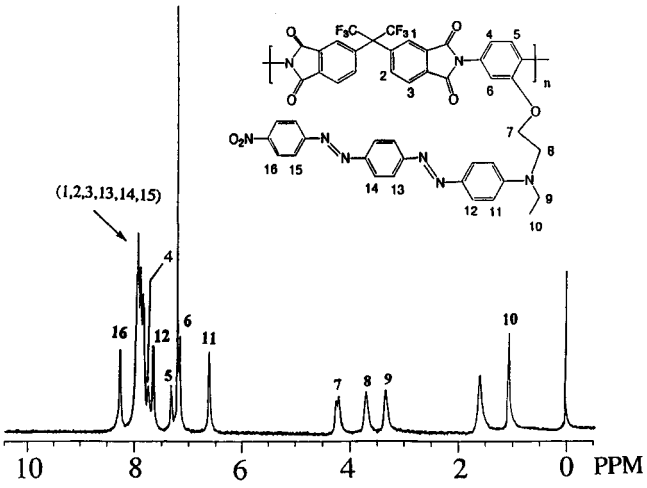

Figure 1. ^{1}H NMR spectrum of **P1**.

Scheme 2. Synthesis of Polyimides

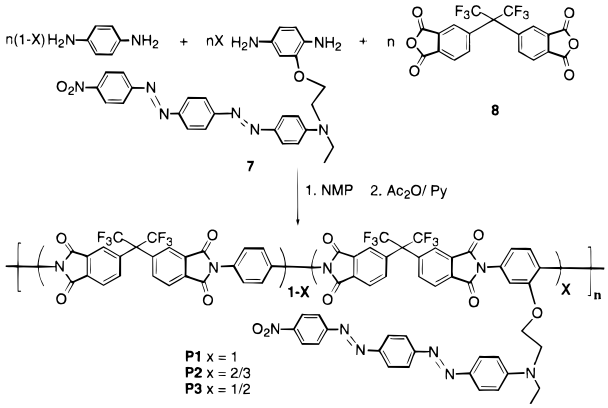

Table 1. Molecular Weights of Polyimides

	X	M_n	M_w	polydispersity
P1	1	27 000	42 000	1.57
P2	2/3	7 300	144 000	1.96
P3	1/2	61 800	123 000	2.00

difference in weight-averaged molecular weight between **P1** and **P2** or **P3**, is due to a technical reason (freshly distilled NMP and freshly recrystallized dianhydride monomer were used in the last two polymers). Optical quality films were cast from tetrachloroethane for NLO studies.

The structures of these polyimides were characterized by spectroscopic techniques. Figure 1 shows the ^{1}H-NMR spectrum of **P1** where the spectral assignments clearly support the proposed structure. Moreover, the ^{1}H NMR analysis permits monitoring of the systematic structural changes throughout the synthesis of the final polymer. The chemical shifts due to NLO chromophore protons do not exhibit much change on going from compound **6** to the final polymer. However, changes in proton chemical shifts of the benzene ring bearing the NLO chromophore are significant. For example, as compound **6** is hydrolyzed to give diamine **7**, three peaks at 6.16, 6.19, and 6.52 ppm, which correspond to the phenylene diamine protons, appeared in the ^{1}H-NMR spectrum. Upon polymerization, these protons shifted downfield to 7.35, 7.75, and 7.20 ppm, respectively, clearly due to conversion of the electron donor diamine to an electron withdrawing diimide on polymerization. ^{1}H-NMR spectra of copolyimides **P2** and **P3** all show one characteristic peak at 7.6 ppm due to the four aromatic protons in the phenyl group from the 1,4-diaminophenylene unit. When the ratio of the 1,4-phenylenediamine increases, as compared to NLO diamine, the magnitude and the integration of the peak at 7.6 ppm increases (Figure 2).

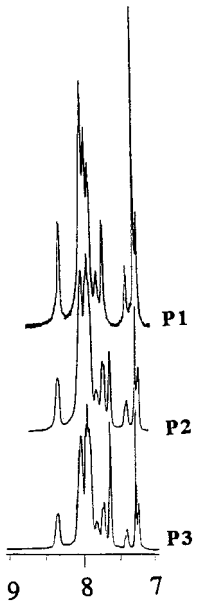

Figure 2. Overlayed ^{1}H NMR spectra for the aromatic regions of **P1**, **P2**, and **P3**.

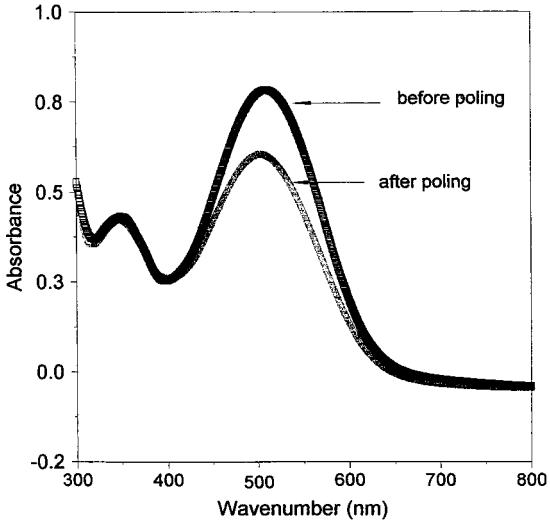

Figure 3. UV−vis spectra of the of **P1** before and after electric poling.

The results of the UV−vis study of this polyimide showed an absorption maximum at 505 nm due to the π-π* transition in the NLO chromophore (Figure 3). After the molecular dipoles were aligned along the direction of the electric field by electric poling, the maximum absorbances were reduced. The order parameters ($\phi = 1 - A_1/A_0$, A_0 and A_1 are the absorbances of the polymer film before and after corona poling) are used to characterize the poling efficiency. Under the conditions of a 4 kV poling voltage applied to the corona needle at 200 °C for 20 min, the order parameter values for **P1**, **P2**, and **P3** were estimated to be 0.24, 0.21, and 0.22, respectively (Figure 3).

Thermal properties of this polyimide were examined by DSC and TGA measurements. DSC studies (Figure 4) indicated that as the loading level of NLO chromophore decreased, the glass transition temperature (T_g) of the polyimide sample annealed at 200 °C increased from 217 to 242 °C (Table 2). Polyimide

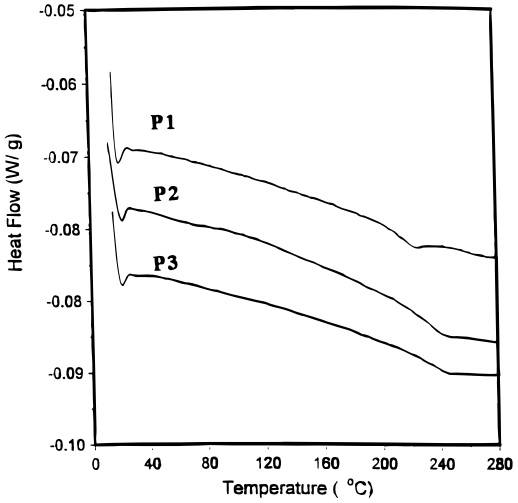

Figure 4. DSC diagrams of polyimides **P1**−**3** with a heating rate of 10 °C/min under a nitrogen atmosphere.

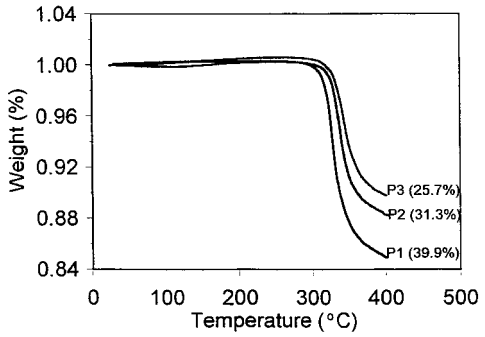

Figure 5. TGA traces of polyimides **P1**−**3** with a heating rate of 10 °C/min under nitrogen atmosphere.

Table 2. Physical Properties of Polyimides

	X	chromophore %	n_{TE}/n_{TM}	T_g (°C)	T_d (°C)	Φ	r_{33} (pm/V)
P1	1	39.9	1.657/1.627	218	300	0.23	35
P2	2/3	31.3	1.634/1.611	238	310	0.21	23
P3	1/2	25.7	1.622/1.599	242	320	0.24	14

backbones are known to decompose above 500 °C. However, TGA traces (Figure 5) showed that these polyimides have decomposition temperatures (T_d) in the range of 300−320 °C, which represents the decomposition of the NLO chromophore from the polymer backbone. These results support the following argument: as the NLO chromophore loading levels increase, the weight loss (weight %) increases accordingly. The TGA studies showed that the decomposition temperature (T_d) of these polyimides was higher than the corresponding glass transition temperatures (300 vs 217 °C for **P1**, 310 vs 238 °C for **P2**, and 320 vs 242 °C for **P3**). This indicates that high-temperature poling for a short term is feasible without damaging the NLO chromophore.

Poling Dynamics and Long Term Stability of the Dipole Orientation. In order to establish a detailed procedure for corona poling, we studied the poling dynamics on the thin films of **PI**. Figure 6 shows the results of the SHG signal as a function of temperature or time. Several important effects can be seen from these results. First of all, large SHG signals can be observed even at room temeperature when the field was turned on. Further heating only helps to increase the SHG signal to a small degree. After the temperature reaches close to the T_g, the SHG signal tends to decrease and eventually disappears if the applying voltage to the

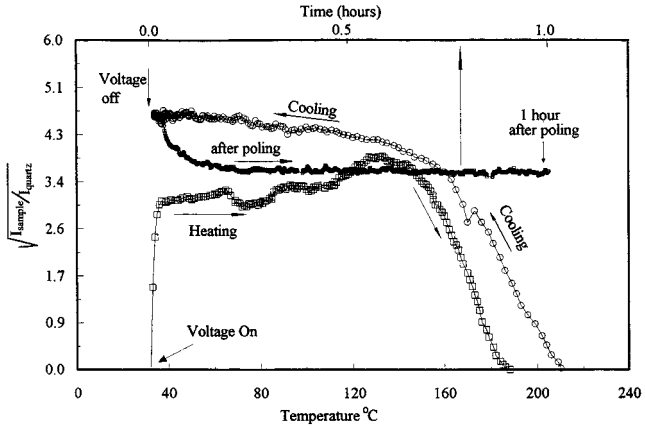

Figure 6. Poling dynamics as a function of temperature and time (see the text).

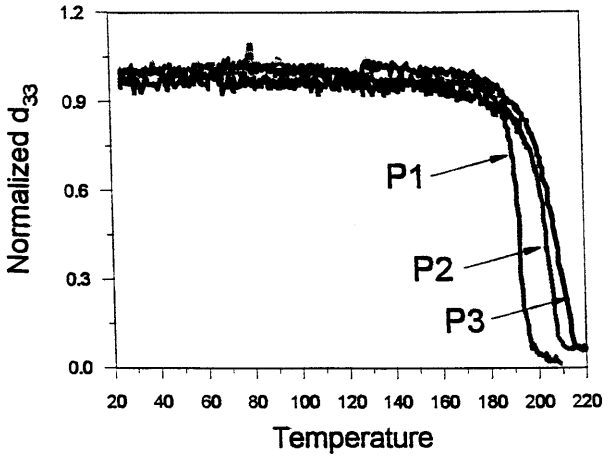

Figure 7. SHG signal of polyimides **P1**−**3** as a function of temperature.

corona needle is fixed. This is clearly related to the two factors: (1) as the temperature increases, the conductivity of the polymer films decreases and thus the effective electric field decreases; (2) high temperature imparts high thermal randomization energy for the NLO dipoles, which can compete with the electric poling field. These effects can be minimized when the temperature is reduced, as shown in the cooling curve. As the cooling occurs, physical aging causes the free volume of the polymer to shrink, thus restricting the chromophore motion and stabilizing the alignment. Because of the physical aging, the conductivity of the polymer film also changes and the surface accumulates more charges than the corresponding heating stage. The SHG signal is higher during the cooling stage than the heating stage. This effect can be seen clearly when the voltage is switched off at room temperature; the initial drop of the SHG signal could well be due to the release of the surface charge. After the initial decay, the SHG signal was maintained at a level identical to the maximum during the heating-up process. These results reveal two points: (1) corona poling can effectively be performed at the temperature near T_g; (2) a finite aging time at the corona poling condition may help to enhance the stability of the dipole orientation.

In addition to the poling dynamic studies, temperature-dependent SHG experiments on prepoled samples were carried out in-situ by monitoring the SHG signal while heating at a rate of 2 °C/min (Figure 7). **P2** and **P3**, which have a higher T_g showed better stability than **P1**. Figure 7 shows that the SHG signal remained

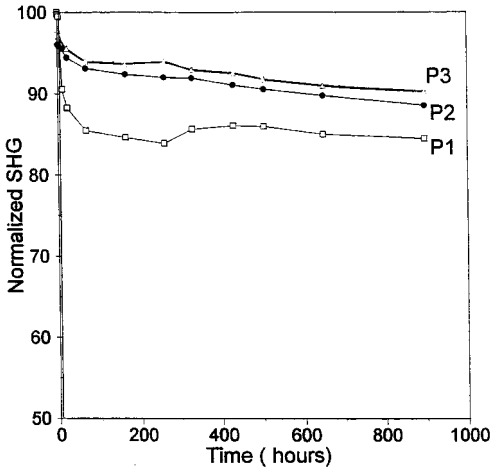

Figure 8. Temporal stability of the SHG signals of **P1**−**3** at 100 °C in the air.

stable for all polymers until reaching the glass transition temperature, where the SHG signal starts to decay rapidly. It completely disappeared as the temperature went above T_g. These results are understandable because the thermal relaxation of oriented dipoles is related to the free volume in the polymer. Once a critical free volume is provided to the oriented dipoles, the relaxation process starts to occur. This critical volume is directly related to the glass transition temperature (T_g) of the polymer; high glass transition temperatures provide better orientational stability.

To probe the long-term stability of the aligned chromophore in the polymer matrix, we monitored the temporal stability of the second harmonic generation (SHG) signals at elevated temperatures. All of the polymers, **P1**−**P3**, displayed no SHG signal decay at room temperature. When the the SHG signal of **P1** was monitored at 100 °C for 900 h, the decay was noticeable at initial stages and then stablized at ca. 82% of its initial value. **P2** and **P3** showed almost identical behavior, since both have a close glass transition temperatures. Their signals stablized at ca. 88% and 90% of their initial value, respectively, after 800 h (Figure 8). These results indicate that these materials are stable enough to withstand the working temperature for long periods.

Optical Properties. Table 2 summarizes the optical properties of the polyimides synthesized. When the chromophore loading levels decreased, the refractive indices (n_{TE} and n_{TM}) decreased accordingly. This interesting feature provides the ability to fine-tune the linear optical properties of these polymeric materials to match the demands for device applications. Since the UV peak absorption of the polymer is at 505 nm, with a tail extending into the infrared, we measured the electrooptic coefficient in the infrared region at 1.3 mm wavelength (using a 5 mW diode laser) to avoid resonant enhancement. A large elecrooptical coefficient (r_{33}) value was obtained for **P1** (r_{33} = 35 pm/V at 1300 nm). When the chromophore loading level was reduced, the value of r_{33} decreased (Table 2). This correlation between r_{33} and the NLO chromophore loading level can be easily explained: the bulk nonlinearity is linearly proportional to the concentration of the NLO chromophores if the chromophore order parameter is similar in different samples.

Conclusion

By expanding our previously developed synthetic approach, polyimides or copolyimides bearing an NLO chromophore with large $\mu\beta$ values were synthesized. These materials exhibit large r_{33} values (35 pm/V at 1.3 μm) and good temporal stability at elevated temperatures (100 °C). It was found that as the length of the NLO chromophore increased, the glass transition temperatures of the polymers decreased due to the plasticization effect. Since the T_g's of these polymers are lower than those of polymers previously reported by us, the stability of the NLO response is poorer than those of other polymers. However, the combination of the large r_{33} values and their reasonable stability puts these materials among the best second-order NLO polymers. Copolymerization of a diamino monomer bearing an NLO chromophore with the more rigid 1,4-diaminophenylene and dianhydride offsets some of the loss in the T_g with a certain tradeoff in optical nonlinearity. Thus, a proper selection of the polymer composition and NLO chromophore is important in obtaining NLO polymers with balanced properties.

Acknowledgment. This work was supported by ONR and the National Science Foundation. Support from the National Science Foundation Young Investigator program is gratefully acknowledged. This work also benefitted from the support of the NSF MRSEC program at the University of Chicago.

References and Notes

(1) Yang, S. Y.; Peng, Z. H.; Yu, L. P. *Macromolecules* **1994**, *27*, 5858.
(2) Yu, D.; Yu, L. P. *Macromolecules* **1994**, *27*, 6718.
(3) Yu, D.; Gharavi, A.; Yu, L. *J. Am. Chem. Soc.* **1995**, *117*, 11680.
(4) Yu, D.; Gharavi, A.; Yu, L. *Macromolecules* **1996**, *29*, 6139.
(5) Chen, T.; Jen, A. K.; Cai, Y. *J. Am. Chem. Soc.* **1995**, *117*, 7295.
(6) Veriest, T.; Burland, D. M.; Jurich, M. C.; Lee, V. Y.; Miller, R. D.; Volsken, W. *Science* **1995**, *268*, 1604.
(7) Wu, J. W.; Valley, J. F.; Ermer, S.; Brinkley, E. S.; Kenney, J. T.; Lipscomb, G. F.; Lytel, R. J. *Appl. Phys. Lett.* **1991**, *58*, 225.
(8) Lin, J. T.; Hubbard, M. A.; Marks, T. J.; Lin, W.; Wong, G. K. *Chem. Mater.* **1992**, *4*, 1148.
(9) Becker, M. W.; Sapochak, L. S.; Ghosen, R.; Xu, C. Z.; Dalton, L. R.; Shi, Y. Q.; Steier, W. H. *Chem. Mater.* **1994**, *6*, 104.
(10) Kaino, T.; Amano, M.; Shuto, Y. In *Nonlinear Optics: Fundamentals, Materials and Devices*; Miyata, S., Ed.; Elsevier Science Publishers B.V.: Amsterdam, 1991.
(11) Wang, X.; Chen, J.; Marturunkakul, S.; Li, L.; Kumar, J.; Tripathy, S. *Chem. Mater.* **1997**, *9*, 45.
(12) Teng, C. C.; Man, H. T. *Appl. Phys. Lett.* **1990**, *56*, 1734.

MA970530O